

17044263_ResearchPaper

anonymous marking enabled

Submission date: 24-Jan-2021 10:37PM (UTC+0000)

Submission ID: 143233926

File name: 17044263_ResearchPaper_2578092_1417138507.pdf (2.61M)

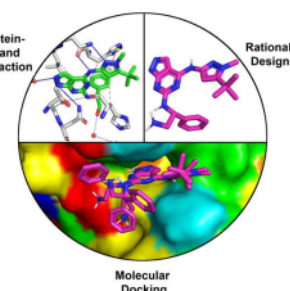
Word count: 8630

Character count: 46949

Modification of a pyrazolopyrimidine derivative to a broad-spectrum Mur Ligase Inhibitor using molecular docking and interaction profiling studies

17044263

ABSTRACT: The rapid emergence of multidrug-resistant strains of bacteria results in an urgent need to develop new medicines. Mur Ligases are an untapped class of enzymes that build the bacterial cell wall peptidoglycan and they are practical targets for dual inhibitors which can slow down the development of resistance. Pyrazolopyrimidine derivatives were found to have excellent inhibitory potency against MurC Ligase, but the compounds were not pursued due to their poor activity against wild-type bacteria. Using recent discoveries in molecular features that correlate with good accumulation in Gram-negatives, this paper presents a suitable site of modification to produce primary amine-containing pyrazolopyrimidine derivatives. The rationally designed molecule has promising binding poses, affinity scores and interaction profiles compared to known inhibitors and a decoy molecule. The findings from this study serve as a cost-effective primer for pre-clinical studies.



■ 1. INTRODUCTION

1.1. The threat of antimicrobial resistance.

75 years ago, Sir Alexander Fleming, the father of antibiotics, gave a prescient Nobel Prize lecture wherein he warned that underdosing penicillin may ‘change the nature of the microbe’.¹ He was describing antimicrobial resistance (AMR) where the use of antimicrobials, which are agents used to treat and prevent bacterial, viral, fungal and parasitic infections, inadvertently selects for organisms with characteristics that favour their survival. More recently, WHO declared AMR as one of the top 10 global public health threat as it reduces the efficacy of antimicrobials which are needed to treat and prevent potentially fatal infections and make chemotherapy and surgery safe.²

Amongst the different types of pathogens, bacteria are especially notorious because there are numerous species resistant against last-resort antibiotics such as carbapenem and colistin.³ In the O’Neill Report in 2014, 700000 deaths were attributed to drug-resistant diseases worldwide.³ These figures are estimated to rise to 10 million by 2050.³ Despite such alarming figures, inherent biological challenges and the perceived lack of profits left a gaping antibiotics discovery void since the 1980s.⁴ In response to this, WHO published a priority list of pathogens to guide research and

development, with the highest priority given to Gram-negative ESKAPE pathogens; carbapenem-resistant Enterobacteriaceae, *Pseudomonas aeruginosa* and *Acinetobacter baumanii*.⁵

1.2. Expanding the spectrum of activity.

Gram-negative bacteria possess an outer membrane made of tightly packed lipopolysaccharides which encapsulates the inner peptidoglycan layer. This effectively prevents passive diffusion of small molecules into the cell.⁶ Furthermore, drugs often fall victim to the highly promiscuous efflux pumps and fail to accumulate inside the cells faster than it can be pumped out, diminishing its activity.⁶

To ameliorate this, a study published by Richter et al⁷ analysed existing antibacterial compounds and summarised the eNTRy criteria, which describe features most strongly correlated with good accumulation in *E. coli*. Those features were the presence of unencumbered primary amines, high rigidity and low globularity. Several molecules were successfully modified to extend their spectrum of activity.^{8,9}

1.3. Targeting Peptidoglycan Synthesis.

Existing antibacterial agents such as penicillin and carbapenem target cell wall peptidoglycan synthesis. Peptidoglycan is a mesh made of crosslinked carbohydrate chains and peptide links, a structural feature exclusive to prokaryotic bacteria and absent

1 - This project is a Type C Data-analysis/data mining project with a word count of 5999 words formatted in the printed style of the Journal of Chemical Information and Modelling (JCIM) by ACS.

in eukaryotic human cells.^{10, 11} It is present in both Gram-positive and Gram-negative bacteria, preventing the bursting of cells due to turgor pressure exerted by the hypertonic intracellular environment.^{10, 11}

A potential drug target is Mur Ligase, a class of ATP-dependent enzymes that play a key role in building and maintaining the peptidoglycan layer.¹¹ MurC, MurD, MurE and MurF take part in step-wise catalytic steps to form the UDP-Mur-NAc-pentapeptides, an essential subunit of the peptidoglycan.^{12, 13} MurC-MurF ligases share highly conserved binding sites between the enzymes as well as among different bacterial species, providing an attractive target for multi-targeting enzymes that can delay the development of mutational resistance.¹⁴

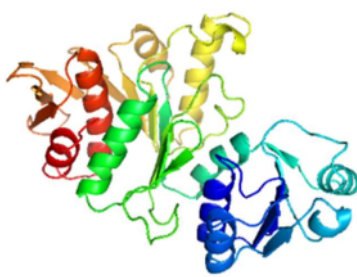


Figure 1. The structure of Chain H of Pae MurC extracted from PDB entry 6x9n. The colour scheme was set as a spectrum of blue to red according to increasing residue number.

1.4. Developing Mur Ligase inhibitors. Despite being an attractive target for antibacterial activity, there are no drugs in the market that can inhibit MurC-MurF ligases¹¹. Nevertheless, a variety of molecules were described to have inhibitory activity against Mur Ligase in the literature.^{11, 15-17} The ATP binding site is a promising target for multitargeting inhibitors as all the Mur ligases use ATP in their catalytic mechanism. Examples of molecules against Mur Ligases that target the ATP binding site include Benzene-1,3-dicarboxylic acid 2,5-dimethylpyrrole derivatives¹⁸ and N-acylhydrazones¹⁹.

This paper takes a focused interest in the pyrazolopyrimidine derivatives published by Hameed et al²⁰ in 2014 which were discovered via high-throughput screening (HTS) of the AstraZeneca compound library. The hit compound

is Compound 1 (AZ8074) which had an IC₅₀ of 1 μM in an enzyme assay against MurC ligase extracted from *Pseudomonas aeruginosa* (Pae).

From the subsequent structure-activity relationship (SAR) campaign, they found Compound 10 (AZ5595) which has an IC₅₀ of 0.001 μM. The molecules were proposed to bind to the ATP binding domain (Residues 119-324) based on the homology model with MurC ligase of *Haemophilus influenzae* and AZ5595-resistant strains were found to develop a single-point mutation on the MurC gene resulting in a Y246C amino acid substitution in its ATP binding domain. However, none of the compounds in the study had good activity against wild-type bacteria.

Despite that, there is renewed attention on the compounds. Seattle Structural Genomics Center for Infectious Disease (SSGCID) deposited the crystal structure of Pae MurC Ligase co-crystallised with AZ5595 and AZ8074 on the Protein Data Bank, as seen in Figure 2 (A) and (B) respectively. The crystallised complexes show molecules binding to the ATP binding domain of Pae MurC. The crystal structure is instrumental in accurately depicting interactions formed by the bioactive protein-ligand complex because the crystallised compounds formed significantly different interactions from the putative ATP binding site determined from homology modelling in the literature²⁰.

To date, there is no structure of Pae MurC Ligase co-crystallised with natural substrates available on the PDB database therefore the exact ATP binding site could not be ascertained. Moreover, as of the writing of this paper, there were no follow-up studies conducted on the pyrazolopyrimidine derivatives.

1.5. In silico techniques in drug discovery. Molecular docking uses geometrical algorithms to model protein-ligand complexes and the interactions formed between the molecules.²¹ It is a powerful technique in computer-assisted drug design and has been widely used to aid hit identification and lead optimisation. It is cost-effective and helps minimise failures in the later stages of the drug discovery process.²² Rapid and automated characterisation of protein-ligand interactions has been made possible using built-for-purpose Java applications.

1.6. Present paper. In the present study, we first interrogate the interactions formed by the crystal structure of Pae MurC Ligase with its inhibitory molecules to rationally design a compound with a broad spectrum of activity based on the eNTRy characteristics.

Following that, molecular docking is used to predict the binding pose and affinity of the modified molecule compared to known strong and weak inhibitors and decoy molecules. Then, we build protein-ligand interaction profiles to compare the interactions formed by the docked ligands and the crystal structure.

By showing that the rationally designed compound has comparable binding affinities, poses and interactions to the crystallised bioactive compound, we hope to suggest a suitable site amenable to modifications that can confer an extended spectrum of activity to pyrazolopyrimidine derivatives. This will guide further pre-clinical studies to expand our weapon arsenal against the threat of antimicrobial resistance.

■ 2. COMPUTATIONAL METHODS

2.1. Characterisation of protein-ligand interaction sites. Protein-ligand complexes were interrogated using visualisation software to identify and illustrate pertinent interactions between both molecules. This step is crucial in the rational modification of AZ5595 with a primary amine and later, comparing the interactions formed by the docked ligands and the crystal structure.

A PDB file containing AZ5595 (PDB entry: 6x9n) was opened using LigPlot+²³ (version 2.2) to generate a 2D schematic diagram of the hydrogen bonds and hydrophobic residues in the ligand's environment. The same file was opened on the web-based Protein-Ligand Interaction Profiler (PLIP)²⁴ to generate a list of interactions and 3D visualisation of the interactions formed which was viewed and edited for clarity with the PyMOL Molecular Graphics System²⁵ (version 2.5.0a0 Open-source by Schrodinger LLC) software. All settings were set at default for PLIP and LigPlot+.

2.2. Molecular design. Structure-activity relationship (SAR) and biochemistry data, namely experimentally determined IC₅₀ and MIC data were extracted from Hameed et al²⁰ as a basis for

modification of the functional groups of AZ5595. The rationale for designing a broad-spectrum antibiotic is based on the eNTRy criteria outlined by Richter et al⁷.

The internal eNTRyway Python program used to calculate a molecule's eNTRyway characteristics was downloaded from the Hergenrother Lab's 'entry-cli' repository on GitHub. From the SMILES notation of each molecule, the Python program calculates each molecule's molecular weight, molecular formula, number of rotatable bonds (RB), globularity (Glob), plane of best fit (PBF) and indicates the presence of primary amine in the molecule.

2.3. Molecular docking. Molecular docking was carried out to predict the interactions formed by protein-ligand complexes. AutoDock Vina 1.1.2²⁶ and its associated graphical interface AutoDockTools 1.5.6²⁷ were used for docking the ligands into the crystal structure of the Chain H of MurC Ligase from *Pseudomonas aeruginosa*.

The program automatically generates conformers by varying its torsion and positions within a specified search space. Then, it uses a hybrid knowledge-based and empirical scoring function to rank the conformers, which considers the number of rotatable bonds and possible steric interactions, hydrophobic interactions and hydrogen bonds formed by each compound.

The program was chosen because it is free for academic use, open-source and a study comparing AutoDock Vina with its predecessor AutoDock 4 showed 100-fold improvement in speed due to the use of multiple CPU cores and better accuracy in binding mode prediction²⁶. Furthermore, an evaluation of the prediction accuracy of sampling power and scoring power of ten commercial and academic docking programs carried out by Wang et al²⁸ found that AutoDock Vina had the best scoring power, which is the correlation between the scoring function and the ranking of binding affinities. The docking protocol, involving preparation of ligand and macromolecule PDBQT files were adapted from the video tutorial made by the software developer²⁹.

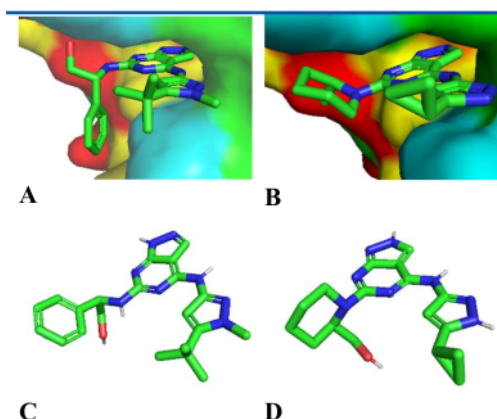


Figure 2. (A) AZ5595 (in green liquorice sticks) bound to the pocket on ATP binding domain on Pae MurC Ligase from PDB entry 6x9n. (B) AZ8074 (in green liquorice sticks) to a nearby site on the ATP binding domain on Pae MurC Ligase from PDB entry 6x9f. The protein is shown as a surface coloured according to properties of amino acid residues. (C) The 3D structure of AZ5595 with ideal, computationally derived geometry. (D) The 3D structure of AZ8074 with an ideal, computationally derived geometry.

2.3.1. Ligand preparation. The main compound we are testing is AZ5595DN2, the rationally designed primary amine-containing pyrazolopyrimidine derivative. Our reference compound is AZ5595, the lead compound identified from the HTS/SAR campaign by AstraZeneca which has the best experimental binding potency (Pae MurC IC₅₀ of 0.001 μM). We will also dock AZ8074, the original hit compound identified from the same campaign, which has a lower binding potency than AZ5595 (Pae MurC IC₅₀ of 1 μM).

Besides that, we designed a Decoy molecule with a similar shape as AZ5595 which will serve as the negative control. We designed it to be a poor binder by replacing the electronegative nitrogen atoms with sulfur atoms which do not form hydrogen bonds and the non-polar tertiary-butyl group replaced with a highly polar chloromethane group. Therefore, we predict that AZ5595 will have greater binding affinities than AZ8074 and Decoy molecule and the docking output of AZ5595DN2 should be comparable to that of AZ5595.

Two groups of ligand files will be prepared for docking. The first group, Group A consist of AZ5595-A, AZ5595DN2-A, AZ8074-A and the

Decoy-A molecule with “ideal” and energetically minimised three-dimensional geometry. The second group, Group B consist of AZ5595-B, AZ5595DN2-B and AZ8074-B in an “alternative” conformation which closely matches the experimentally derived geometry. The 2D and 3D structures of seven ligands used for docking described below are shown in Table 1.

2.3.2. Group A: Molecules with Ideal Geometry.

The ideal SDF files of the ligands AZ5595 and AZ8074 were downloaded from the PDB website from PDB entries 6x9n and 6x9f respectively. The files contain the “ideal” coordinates of atoms, which are calculated by a software based on the known covalent geometry. They are favoured for modelling because the deviations from ideal geometry present in experimental structure determinations (e.g. X-ray crystallography) are minimised³⁰.

A set of 16 low-energy conformers of all the ligands were generated, using the random, low energy bias algorithm and the MMFF94s+ forcefield. From the 16 conformers, the lowest energy conformer in the set was selected for docking, individually viewed in PyMOL to ensure none of the atoms is clashing and the bond angles are sensible and then saved as a PDB file for processing in AutoDockTools.

2.3.3. Group B: Molecules with Alternative Geometry.

Apart from molecules with ideal geometry, we will be docking molecules with “alternative” conformations because there is a marked difference in the predicted best docking pose from minimised conformers of the ligands and the bound conformation in the crystal structure.

As seen in Figure 2(C), the phenyl ethanamine moiety in the idealised geometry of AZ5595-A is co-planar or “in-plane” with the pyrazolopyrimidine scaffold, while the same group in the experimentally derived model in Figure 2(A) is folded “out-of-plane” from the pyrazolopyrimidine scaffold. It is important to differentiate between the rotational angles of the phenyl ethanamine group because in the crystal structure the phenyl folds closer to the surface of the enzyme and forms a Van Der Waals (VDW) interaction with Histidine-288. This interaction will be lost if the phenyl ethanamine group lies flat and

interacts more with the solvent. Moreover, different torsion angle of the piperidine group can be seen in the crystal structure and the ideal geometry of AZ8074, as seen in Figures 2(B) and 2(D) respectively.

Therefore, additional conformers of the ligands were docked to see whether the starting conformers will influence the docking poses and the binding affinities. AZ5595-B and AZ5595DN2-B are out-of-plane conformers of AZ5595 and AZ5595DN2 respectively while AZ8074-B is the experimentally determined model of AZ8074. The model files were downloaded from the same PDB entries as above.

Each PDB file was imported into AutoDockTools. The software prepares the ligand file so that it has the right atom types, compute Gasteiger partial charges, merge non-polar hydrogens, detect aromatic carbons and sets up the torsion tree. The rotatable bonds on each file are manually selected before the ligand is exported as a PDBQT file.

2.3.4. Macromolecule Preparation. The co-crystallised structure of MurC Ligase from *Pseudomonas aeruginosa* with the hit inhibitor AZ5595 from SSGCID was obtained from the PDB website (PDB entry: 6x9n). The structure contains 8 identical chains, A to H, non-protein structures such as water, valine, dimethyl sulfoxide (DMS), ethanediol and chloride ions and one AZ5595 bound to every chain. From the eight chains, chain H was arbitrarily selected for docking and the non-protein components were removed.

AutoDockTools version 1.5.6. was used to add polar hydrogens, Gasteiger partial charges and atom

types to the selected protein file. The search space for docking was selected by placing the grid box around the binding site of AZ5595, setting the scale as 1 Å and the box size to 28 x 28 x 28 to ensure the box size is under 25000 Å. The size of the search space influences the time to generate the output and the ability for the search algorithm to find the correct bound conformation.

2.3.5. Docking procedure. A configuration file was made defining the variables for molecular docking, namely the file containing the ligand, the receptor, the output file, the log file and the size and coordinates of the search space and exhaustiveness of the search. Exhaustiveness was set as “8”, which is the number of independent runs carried out by the program to modify the conformations, optimise and select the binding poses. This will increase the likelihood of finding the correct conformation at the global energy minimum. Besides that, all the other parameters are set at default.

In the log file, predicted binding affinity is measured as kcal/mol, as the program was developed in the USA. The values can be converted into the SI unit kJ/mol by multiplying the values by 4.184. The program also generates an output PDBQT file with the docked conformations, which can be overlaid with the receptor file (Pae MurC Chain H) and inspected together in PyMOL. Figure 3(A) shows a PDBQT file containing AZ5595DN2-B before docking and Figure 3(B) shows an example of how multiple conformations of AZ5595DN2-B are docked on the protein.



Figure 3. (A) shows the conformation of AZ5595DN2-B before docking. (B) shows the top 3 predicted poses of AZ5595DN2-B after docking with AutoDock Vina.

Table 1. A table showing the 2D structure, 3D structure and IC₅₀ data against *Pseudomonas aeruginosa* extracted from the paper by Hameed et al. The minimised energy of the conformers is given below the 3D structure if available.

Name	Conformation of phenyl group	2D Structure	3D Structure	Pae IC ₅₀ (μM)
AZ5595DN2-A	In-plane, minimised			- Energy: -43.8 kcal/mol
AZ5595DN2-B	Out-of-plane, minimised	Same as above		- Energy: -40.9 kcal/mol
AZ5595-A	In-plane, minimised			0.001 Energy: -50.2 kcal/mol
AZ5595-B	Out-of-plane, minimised	Same as above		- Energy: -43.3 kcal/mol
AZ8074-A	Minimised			1.0 Energy: -96.7 kcal/mol
AZ8074-B	Unminimised	Same as above		- Energy: unknown
Decoy-A	Minimised			- Energy: 61.7 kcal/mol

3. RESULTS AND DISCUSSION

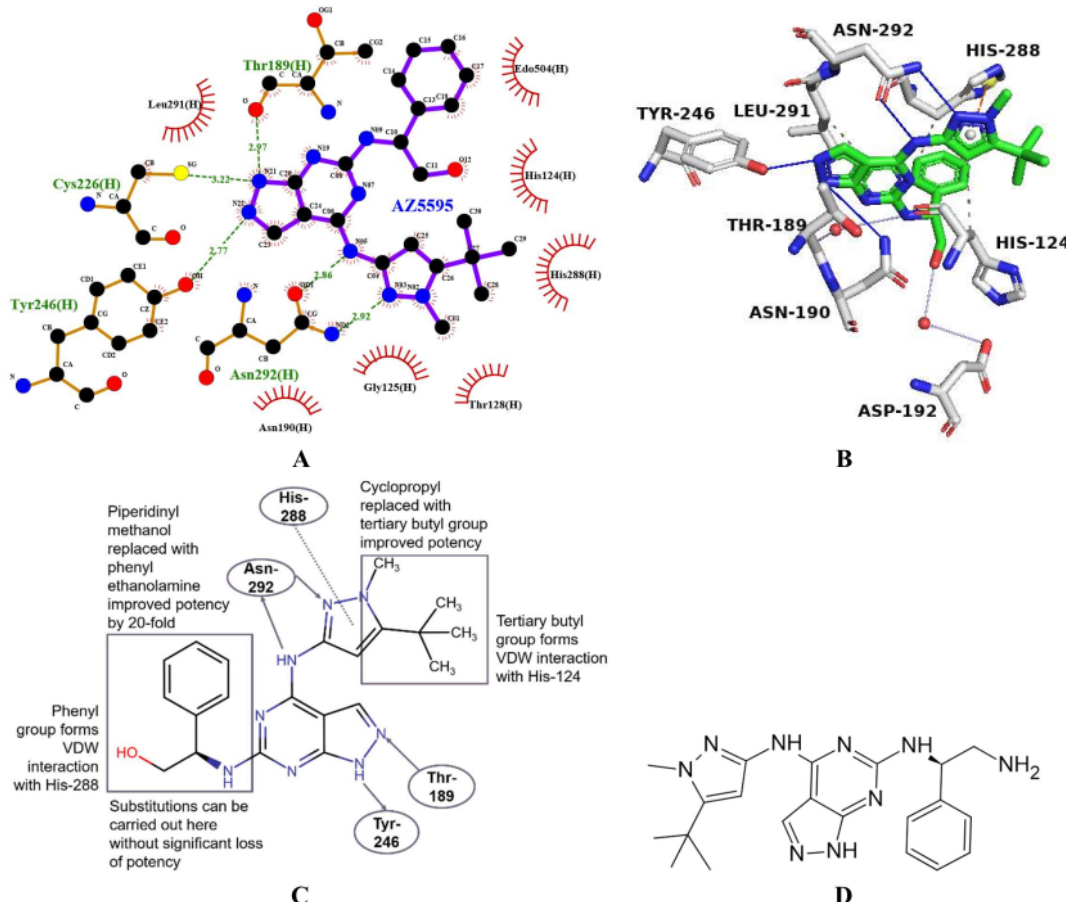


Figure 4. (A) The 2D schematic diagram of the protein-ligand interactions formed by AZ5595 (as black carbons with purple bonds) with Chain H of Pae MurC Ligase generated by LigPlot+. The residues forming polar interactions are shown as ball and sticks while the residues forming hydrophobic contacts are shown as red spoked arcs. (B) The 3D interaction profile generated by PLIP, viewed on PyMOL. AZ5595 is shown as green liquorice sticks and the interacting residues are shown as grey liquorice sticks. (C) Illustration showing the 2D structure of AZ5595, the interactions identified and additional information from the SAR studies conducted by Hameed et al for the rational design of a new molecule. Blue arrowheads are pointing towards hydrogen bond acceptors and green dotted lines illustrate pi-pi interactions. (D) Modified structure of AZ5595, dubbed AZ5595DN2.

3.1. Molecular design using protein-ligand interactions, SAR data and eNTRy criteria.

3.1.1. Protein-ligand interactions and SAR data.

Most of the hydrogen bond interactions are formed by the pyrazolopyrimidine scaffold. The crystal structure in Figure 2(B) and (C) shows the pyrazolopyrimidine scaffold in both AZ5595 and AZ8074 forms a deep pocket in the enzyme, therefore it can be surmised that the scaffold is important for binding to the protein. From Figure 4

(A) and (B), we can see that the hydroxy side-chain on Asparagine-292 forms a hydrogen bond with both the nitrogen on the monocyclic pyrazole ring and the secondary amine linker. Besides that, the phenyl group on Tyrosine-246 forms a hydrogen bond with one of the nitrogen on the pyrazole ring of the pyrazolopyrimidine scaffold. This could explain the Y246C gene mutation observed in AZ5595-resistant strains. Both programs also identified a hydrogen bond between the hydroxy

group on Threonine-189 with another nitrogen on the same bicyclic heterocycle.

Furthermore, PLIP showed that Histidine-288 formed pi-cation interaction with the monocyclic pyrazole ring and hydrophobic interactions with the tertiary-butyl group, and this is consistent with the proximity of the red arc of Histidine-288 with the tertiary-butyl group identified by LigPlot+. It is worth mentioning that Hameed et al²⁰ found that the tertiary butyl group gave the molecule a significant increase of potency. Threonine-189 was found to form a water bridge with the secondary amine linker between the scaffold and the phenyl ethanolamine moiety.

The hydroxy group on the phenyl ethanolamine moiety was not found to form hydrogen bond interactions with any of the residues, other than the possible hydrophobic interaction with the nearby Histidine-124 and the water bridge formed with Asparagine-192. This is expected considering the phenyl ethanolamine group is more

exposed to the solvent compared to the pyrazolopyrimidine core, as seen in Figure 2(A). This corresponds with Hameed et al's²⁰ findings that the phenyl ethanolamine group is open to substitutions without significant loss of potency.

Therefore, the best location to modify the structure and add a primary amine group without interfering with the interactions formed by the original hit compound AZ5595 is by replacing the hydroxy group with a primary amine in the phenyl ethanolamine moiety, as shown in Figure 4(D). Due to the similarity with existing compounds, it is feasible to synthesise the following molecule from commercially available compounds and laboratory-derived building blocks.

Furthermore, we expect the perturbation to the interactions to be minimal, considering NH₂ and OH share similar hydrogen bond-forming capabilities. Besides that, their molecular weights are at 17 and 16 g/mol respectively, thus the two groups are not sterically dissimilar.

Table 2. A table comparing the eNTRy characteristics of the molecules from the AstraZeneca HTS/SAR study and similar molecules from the study done by the Hergenrother Lab. The data for Tigecycline, Chloramphenicol, PTK-0796 and 4-28-a has been reproduced from the paper by Richter et al.

Name	Primary Amine	Mol Wt	Rotatable Bond (≤ 5)	Globularity (<0.25)	PBF	Accumulation (nmol/10 ¹² CFUs)	Spectrum of activity
AZ5595DN2	Yes	405	7	0.11	1.06	Unknown	Unknown
AZ5595	No	406	7	0.11	1.05	Unknown	No WT MIC
AZ8074	No	354	5	0.10	0.93	Unknown	No WT MIC
Decoy	No	431	7	0.16	1.07	Unknown	Unknown
Tigecycline	No (Secondary)	586	7	0.23	1.32	Unknown	Gram-negative
Chloramphenicol	No	323	6	0.15	0.88	709	Gram-negative
PTK-0796	No (Secondary)	557	7	0.14	1.27	Unknown	Gram-negative
4-28-a	Yes	327	8	0.15	0.99	895	Unknown

Mol Wt = Molecular Weight, CFU = colony forming unit, PFB = plane of best fit, WT = wild-type

3.1.2. eNTRy characteristics for broad-spectrum activity. Richer et al have described the eNTRy criteria, which correlates with increased accumulation in Gram-negative bacteria. Good accumulators were found to have sterically unhindered ionisable Nitrogen, favouring primary amines, low three-dimensionality (Globularity of less than 0.25) and rigid (less than 5 rotatable bonds). The table above compares the eNTRy characteristics of AZ5595, AZ5595DN2 and

AZ8074 with the molecules generated by the Hergenrother Lab and existing antibiotics with share similar characteristics as the AZ inhibitors with good accumulation or known Gram-negative activity.

From the eNTRyway program calculations in Table 2, AZ5595DN2 was found to meet the primary amine and globularity criteria. However, it has 7 rotatable bonds, which is more than the rigidity limit of 5 rotatable bonds. However, the

study also found several molecules with more than 5 rotatable bonds, namely Tigecycline, Chloramphenicol, PTK-0769 and 4-28-a as having good accumulation and/or Gram-negative activity. Considering there is strong rationale supporting the design of the structure based on experimental SAR studies, AZ5595DN2 was chosen as the primary focus of this project.

3.2. Binding Affinity and Visual Inspection of Molecular Docking Output. The binding affinities were viewed in conjunction with the docked poses on PyMOL to verify whether the predicted poses correlate well with the established binding location and pose on the Pae MurC Ligase crystal structure. Images of the top three poses, ranked 1st, 2nd and 3rd and their corresponding binding affinity values are shown in Table 3 below.

Table 3. A table containing images of the top three poses of ligands with their corresponding binding affinities in kcal/mol given below the images. The docked conformations are shown as magenta liquorice sticks, the crystallised AZ5595 is shown as green liquorice sticks and the Pae MurC Ligase is shown as cyan cartoon structure. A more negative binding affinity value indicates greater binding affinity value or magnitude.

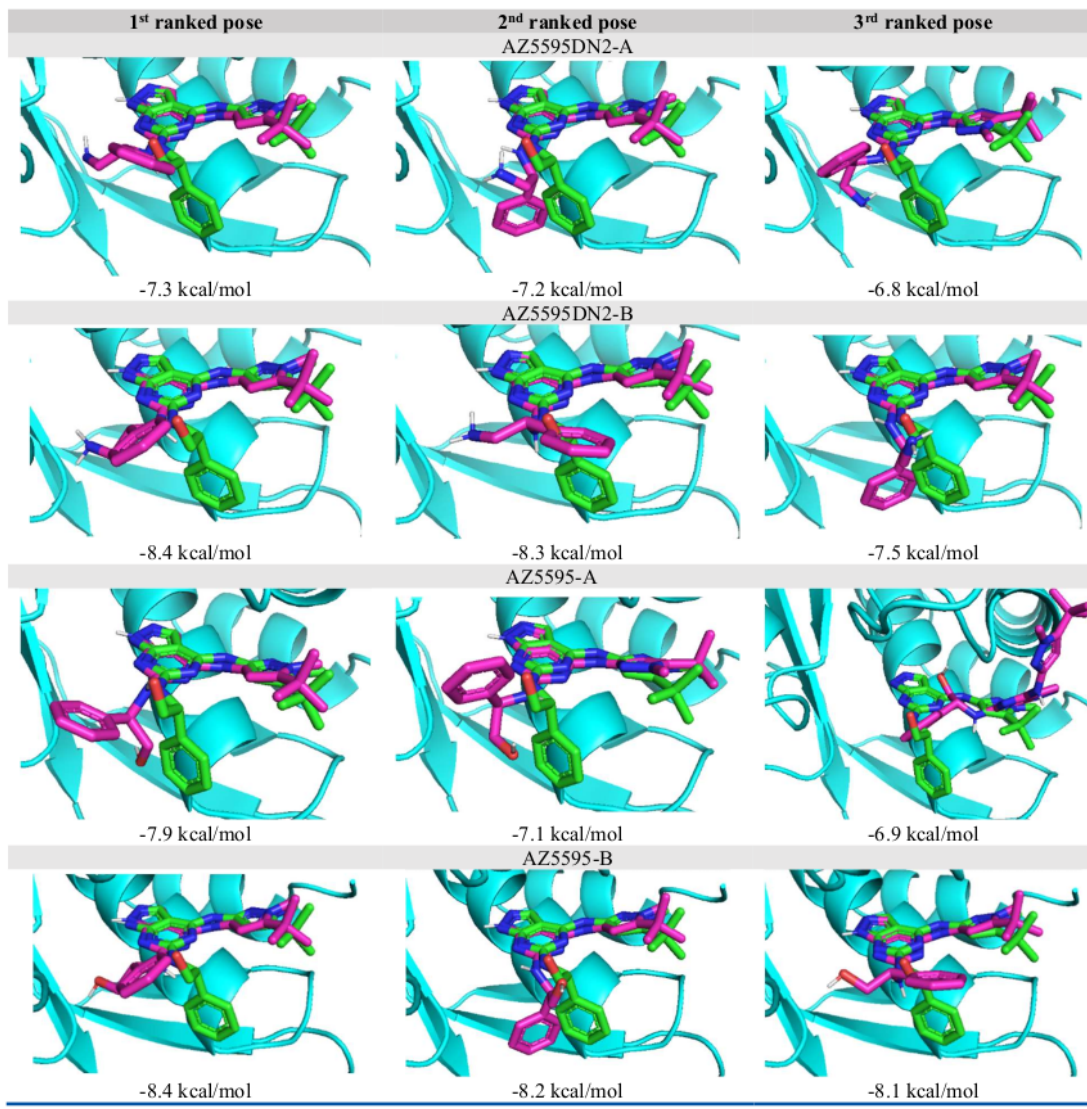
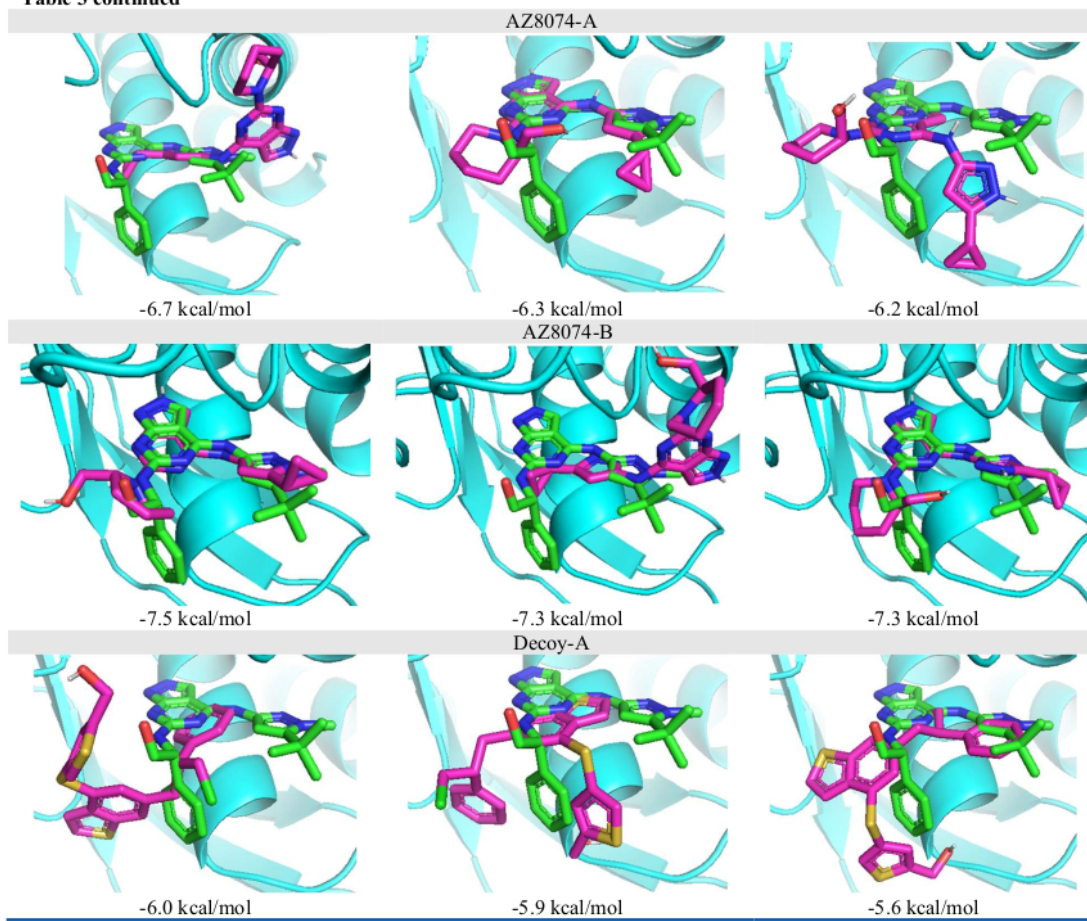


Table 3 continued



3.2.1. General binding affinity trend of the best-ranked pose. The binding affinity of the 1st pose is used as the first point of comparison because it is the conformation that corresponds with the minimum of the affinity scoring function. Generally, the trend seen in the binding affinities of the compounds predicted by AutoDock Vina is in line with the hypothesis outlined in Section 2.3.1.

From Table 3, both AZ5595-A and AZ5595-B yielded the highest binding affinity values compared to the rest of the ligands, at -7.9 and -8.4 kcal/mol respectively. Promisingly, it is followed by the rationally designed primary amine-containing compound AZ5595DN2-A and AZ5595DN2-B, at -7.3 and -8.4 kcal/mol each. As expected, the poor binder AZ8074-A and AZ8074-B gave low binding energies of -6.7 and -7.5

kcal/mol respectively. Furthermore, Decoy-A, which is predicted to be a poor binder by design, produced poses with the lowest free energy of binding of -6.0 kcal/mol.

While there are prevailing concerns about the accuracy and reliability of molecular docking and binding affinity predictions^{31, 32}, we were able to compare the binding affinity calculated by AutoDock Vina and the experimental potencies of the ligands to determine the validity of the computational output. As explained above, AZ5595, the molecule with the high potency against Pae MurC (IC_{50} of 0.001 μ M) has a higher binding affinity than AZ8074, the molecule with the low potency against Pae MurC (IC_{50} of 1 μ M). This suggests that the higher experimental potency AZ5595 correlates with the number and strength of

the interactions the molecule formed with the Pae MurC protein residues, and this was accurately predicted by AutoDock Vina's scoring function. Additionally, the poor binding affinity of our negative control, Decoy-A solidifies our confidence in the in-silico predictions.

Furthermore, it was observed that Group B ligands gave rise to higher binding affinity values compared to Group A ligands. The variation in binding affinity values of individual ligands can be explained by the non-deterministic nature of the docking algorithm.³³ Nevertheless, we believe that this should not affect the validity of our findings since the same trend is observed in both Group A and Group B docking iterations.

3.2.2. Comparing binding affinity and poses of AZ5595DN2 and AZ5595. AZ5595DN2 is the primary-amine containing rationally designed compound while AZ5595 is the AstraZeneca lead compound with $0.001\mu\text{m}$ IC_{50} against Pae MurC Ligase.

Overall, the predicted binding affinities of the primary amine-containing compound AZ5595DN2 have similar, albeit slightly lower magnitude compared to that of AZ5595 in both Group A and Group B docking experiments. For example, the top three poses of AZ5595DN2-B have binding affinities of -8.4, -8.3 and -7.5 kcal/mol while AZ5595-B have binding affinities of -8.4, -8.2 and -8.1 kcal/mol.

This could suggest that AZ5595DN2 formed fewer interactions or the interactions are formed over longer distances than AZ5595. Protein-ligand interaction profiling needs to be carried out on the docked molecules to illustrate the differences in binding interactions. As explained in Section 3.1.1., we do not expect significant changes, considering NH₂ and OH share similar physical and chemical properties.

Furthermore, all top poses of AZ5595DN2 showed good overlapping of the pyrazolopyrimidine scaffold and the tertiary-butyl group (magenta) with AZ5595 in the crystal structure (green). Besides that, the same can also be said about redocked AZ5595, except for the 3rd ranked pose of AZ5595-A where the compound showed a starkly different binding pose. Overall, we can see that the docked ligands with the

pyrazolopyrimidine scaffold that align well with the crystal structure have higher binding affinities compared to the ones with alternative binding poses. For example, the 1st ranked pose of AZ5595-A with a binding affinity of -7.9 kcal/mol overlaps well with the crystallised AZ5595, while the 3rd ranked pose with a binding affinity of 6.9 kcal/mol does not align well with the crystal structure.

This illustrates the importance of the scaffold in forming efficient interactions with the protein molecule. A large degree of overlapping in the scaffold also validates the ability of the algorithm to accurately recognise and reproduce the binding site of AZ5595 which had been experimentally determined by X-ray crystallography.

However, some variation could be observed in the rotation of the phenyl group and none matched the torsional angle in the crystal structure exactly. AutoDock Vina favoured the phenyl group lying flat or in-plane with the pyrazolopyrimidine core, ranking them higher than the out-of-plane conformations in both Group A and Group B docking experiments.

For instance, in AZ5595DN2-B, the poses with the in-plane conformation of phenyl group were ranked 1st and 2nd, with binding affinities at -8.4 kcal/mol and -8.3 kcal/mol respectively, and the poses with an out-of-plane conformation ranked 3rd with a binding affinity of -7.5 kcal/mol. The same can be said for AZ5595. For instance, the 1st and 3rd ranked pose of AZ5595-B showed an in-plane rotation and the out-of-plane conformation was not found in the top three docking poses in AZ5595-A.

Differences in the conformation of the docked ligands and the crystal structure are expected because AutoDock Vina explores the different bond rotation and torsion angles to find the conformation in the global energy minimum. This simply implies that the Van Der Waals interaction between the out-of-plane phenyl group and Histidine-288 does not overcome the energy penalty for rotating the phenyl group closer towards the pyrazolopyrimidine core and Pae MurC Ligase.

It is difficult to ascertain the significance of this, as several studies in the past have described the disparity between docked poses of low energy conformers and the actual conformation in protein-ligand complexes^{34, 35}, yet another paper showed a

preference for local minimum conformations for binding of small molecules to proteins³⁶.

Nevertheless, this could suggest that the phenyl and hydroxy or amino groups in AZ5595 and AZ5595DN2 respectively are less likely to be involved in interacting with the residues on the ATP binding domain of Pae MurC Ligase. All in all, there is good evidence that the site can be considered for further rational modification.

3.2.2. Comparing binding affinity and poses of AZ5595DN2 against AZ8074 and Decoy molecule. AZ8074 is the AstraZeneca hit compound with 1 μM IC₅₀ against Pae MurC Ligase while the Decoy molecule is a poor binder-by-design with a similar size and shape as AZ5595.

Favourably, the binding affinity of AZ5595DN2 is consistently higher than that of AZ8074 and the Decoy molecule. For instance, in Group A docking where the compounds have ideal and energetically minimised geometry, the top three poses of AZ5595DN2-A have binding affinities of -7.3, -7.2 and -6.8 kcal/mol. Meanwhile, AZ8074-A have binding affinities of -6.7, -6.3 and -6.2 kcal/mol and Decoy-A have binding affinities of -6.0, -5.9 and -5.6 kcal/mol. This could suggest that the substitution of the hydroxy group with the primary amine does not significantly perturb the interactions formed with the original scaffold and will not theoretically affect its potency.

Moreover, we can expect the low binding affinity values for AZ8074 because the predicted pose of AZ8074 was less likely to align well with AZ5595 in the crystal structure. For instance, we can see in Table 3 that the 1st ranked pose of AZ8074-A and the 2nd ranked pose of AZ8074-B occupies a significantly different binding site than the crystallised AZ5595. They would likely form different or weaker interactions with different residues in the pocket. Additionally, this could

suggest the role of the tertiary-butyl group and the out-of-plane phenyl ethanolamine group in AZ5595 as stabilising anchors, forming interactions with the surrounding residues while allowing the pyrazolopyrimidine scaffold to enter the binding pocket with the correct orientation and ultimately, elicit its inhibitory effect.

Finally, the low binding affinity formed by Decoy-A suggests that the docking program did not find energetically favourable poses that could form strong interactions with the protein side-chain residues within the designated search space. Moreover, none of the top three poses matches the crystal structure of AZ5595. This establishes that the binding site and the interactions formed by AZ5595 and the protein residues are specific to the pyrazolopyrimidine scaffold and other derivatives which share its properties.

3.3. Binding Interactions and Distance

Profile. The 2D protein-ligand interaction maps were generated using LigPlot+ to ascertain the types of interactions with Pae MurC residues formed by the crystal structure, which of these were shared by the docked ligands and their corresponding distances. Static images of the interaction maps are included in the Supporting Information.

The bond distances were extracted into Table 4 below and made into a radar map (Figure 5) to graphically illustrate the difference in distances, with the points in the centre of the radar map representing shorter bond distances with the residues. Dashes signify that any contacts below 4 Å with the particular residue was not found. However, each ligand may interact with other residues, which can be seen more clearly in the 2D interaction maps. The numbering of nitrogen is based on the LigPlot+ numbering on crystallised AZ5595 in Figure 2(A).

Table 4. The interactions formed by the pyrazolopyrimidine scaffold in the crystal structure, the distances of the bonds formed by the ligands to the residues and their corresponding binding affinities. N3, N5, N22, and N21 are nitrogen atoms on the compounds that form contacts with the residues.

Ligand	Conformation	Affinity (kcal/mol)	Binding Distance (Å)				
			ASN292 (NH2) – N3	ASN292 (O) – N5	TYR246 – N22	THR189 – N21	
Crystal AZ5595	Out-of-plane	-	2.92	2.86	2.77	-	2.97
AZ5595-A	In-plane	-7.8	3.02	3.05	-	3.26	3.06
AZ5595-B	Out-of-plane	-8.2	2.97	3.02	3.32	-	3.03
AZ5595DN2-A	In-plane	-7.3	3.31	3.16	2.83	-	3.16
AZ5595DN2-B	Out-of-plane	-7.5	3.04	3.07	-	3.37	3.05
AZ8074-A	Ideal	-6.7	3.15	3.11	-	-	-
AZ8074-B	Model	-7.5	-	3.02	2.84	-	-
Decoy	Ideal	-6.0	-	-	-	-	-

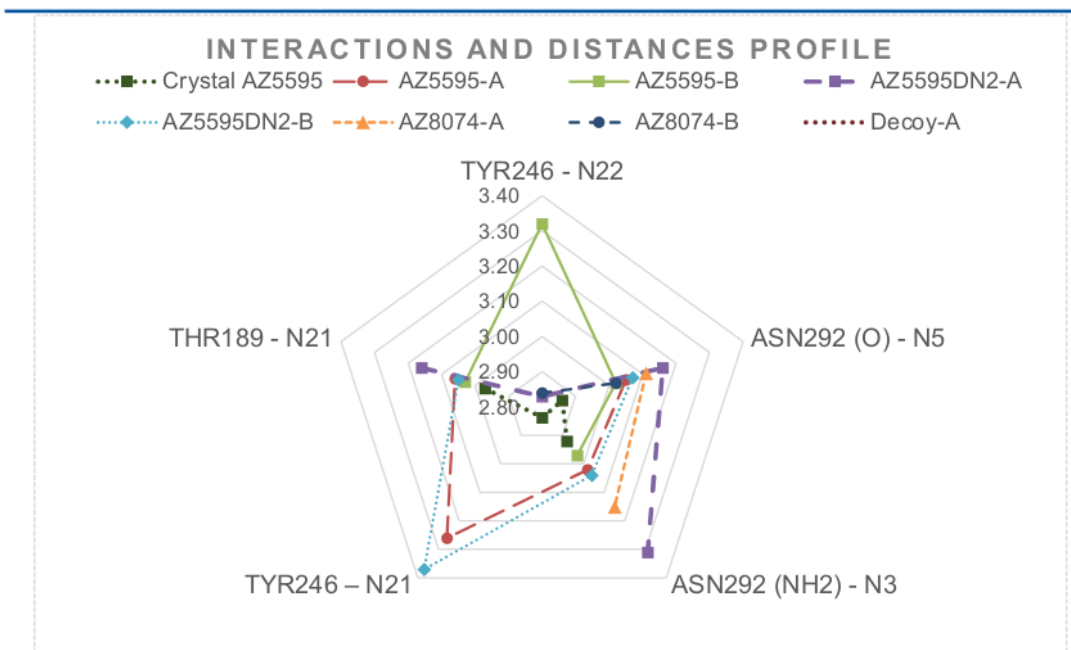


Figure 5. A radar map illustrating the distances of the bonds formed compared to the interactions formed in the crystal structure in the centre.

As summarised in Table 4, the pyrazolopyrimidine scaffold of crystallised AZ5595 formed hydrogen bonds with Asn-292, Tyr-246 and Thr-189. The distances formed are 2.92 and 2.86 Å to Asn-292, 2.77 Å to Tyr-246 and 2.97 Å to Thr-189, which are collectively shorter compared to the bond distances formed by the docked ligands. From Figure 5, we can see that the crystallised AZ5595 is at the centre of the map, signifying that it forms the closest contacts with the MurC residues. Meanwhile, the

docked molecules are further away from the centre as they form interactions over longer distances than the crystallised structure.

Promisingly, the interaction profile shows that AZ5595DN2 forms the same contact points as AZ5595 in the crystal structure, albeit over longer distances. For example, 1st ranked pose of AZ5595DN2-A forms two hydrogen bond with Asn-292 over distances of 3.31 and 3.16 Å. Besides that, it forms hydrogen bonds with Tyr-246 and

Thr-189, over distances of 2.83 and 3.16 Å respectively.

We can also see that AZ5595DN2 outperforms AZ8074 and the Decoy molecule. For instance, the 1st ranked pose of AZ8074-A shares only two hydrogen-bonds with the crystal structure, namely with the Asn-292 and Tyr-246, over distances of 3.15 and 3.15 Å respectively. Furthermore, Decoy-A did not share any of the hydrogen bond interactions with the residues as that of the crystal structure.

Large similarities between AZ5595 and AZ5595DN2 means that replacing the hydroxy group on AZ5595 with a primary amine does not disturb the pertinent interactions formed with the enzyme. We have confidence that the binding potency of the compound will not be significantly decreased by the modification. However, it is worth to note the observed differences of the contact points with Tyr246. They can be explained by the different tautomeric forms of the molecule (Figure 6(A)) as well as the fact that Tyr246 can act as both hydrogen bond donor and acceptor (Figure 6(B)).

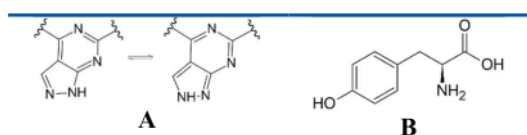


Figure 6. (A) The tautomeric forms of pyrazolopyrimidine which could give rise to different nitrogen atoms interacting with Tyr-246. (B) The 2D structure of the amino acid residue Tyrosine. The phenol group can act as both a hydrogen bond donor or a hydrogen bond acceptor.

3.4. Limitations of the study Molecular docking, while an essential component of computer-assisted drug discovery, comes with its own set of limitations. Firstly, water molecules can form water bridges between the ligand and the receptor and play a role in aligning the ligand in the binding site. However, water molecules are typically removed when preparing macromolecule files for docking to ease computational burden and remove any potential confounding effects on direct protein-ligand interactions. Besides that, AutoDock Vina uses a united-atom scoring function which involves only heavy atoms, meaning hydrogens are only used to assign atom types and its positions in

the output are arbitrary.³³ Therefore, even if water molecules are included in the docking receptor file, only the positions of oxygen molecules will be accurate.

Moreover, in the input files, the ligands are flexible, but Pae MurC Ligase Chain H was treated as a rigid receptor. This is not a realistic representation as proteins are flexible and both protein side-chain residues and the ligand can rotate and conform to each other. Despite that, this particular molecular docking was conducted using the experimentally-determined crystal structure of Pae MurC with the inhibitory AZ5595 bound to it, meaning the positions of the protein side chains should already be in its inactivated, induced-fit state in the presence of the inhibitor, at a resolution of 2.25 Å. This should provide a degree of confidence in their interactions with the docked ligands in this study.

Nevertheless, molecular dynamics (MD) simulations should be carried out in the presence of water molecules to produce realistic binding poses as a follow-up to molecular docking studies. MD is a common computer-assisted drug discovery technique to evaluate the stability of the protein-ligand complexes as it measures the bond distance and energy fluctuations for a specified duration.

■ 4. CONCLUSION

Various investigations have been published describing molecules that can inhibit Mur Ligases yet none have successfully entered the clinic. Hameed et al conducted high-throughput screening against a library of compounds by AstraZeneca and their SAR campaign yielded pyrazolopyrimidine derivatives with sub-micromolar inhibitory activity against MurC Ligase and efflux-mutant bacteria. However, none of these molecules was found to have sufficient activity against wild-type *E. coli* and *P. aeruginosa*. From our experiments, we have shown that the pyrazolopyrimidine derivatives can be rationally designed using the principles of eNTRy characteristics outlined by Richter et al which has successfully been used to modify molecules from Gram-positive-only to broad-spectrum antibiotics.

We have used AutoDock Vina to dock flexible ligands into rigid Pae MurC Ligase and used PyMOL, PLIP and LigPlot+ to study the conformations and bonds formed within the protein-ligand complex. We found evidence that substitution of the hydroxy group on AZ5595 with a primary amine will not interrupt existing binding pose and interactions with Pae MurC Ligase. Two sets of docking experiments with AZ5595DN2 have consistently shown good overlapping of its core with the experimentally determined crystal structure, promising predicted binding affinity and interactions within the protein-ligand complex compared to molecules with weaker potencies such as AZ8074 and the poor binder-by-design Decoy molecule. Thus, we have confidence that the molecule will have similar *in vitro* binding affinity and potency against the antibacterial target as AZ5595, as well as having characteristics that correlate with increased accumulation in Gram-negative bacteria.

Together with our computational analysis, existing SAR data and binding interactions support the importance of conserving the pyrazolopyrimidine scaffold, the phenyl group and the tertiary butyl groups to maintain high potency against MurC Ligase. Therefore, we posit R1 (Figure 7) as a suitable site of further modification to build a library of rigid, flat and primary amine-containing compounds for further studies.

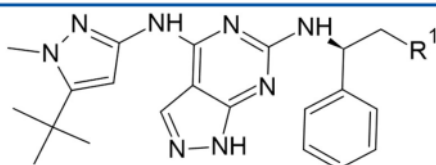


Figure 7. The 2D Structure of AZ5595 with R1 as the promising site of modification.

4.1. Future Work Firstly, chemical synthesis of AZ5595DN2 should be carried out to provide the necessary samples for *in vitro* studies. Due to similarity with AZ5595, we found that it is feasible to synthesise AZ5595DN2 from commercially available compounds and laboratory-derived building blocks.

Besides that, as mentioned before, we should employ computationally intensive molecular dynamics simulations to study the formation of protein-ligand complexes that is representative of their real-world behaviour.

Moreover, the compounds should be docked to MurC Ligase of other bacterial species such as *Haemophilus influenzae* and *Acinetobacter baumanii* to improve our confidence on the molecule's inhibitory activity against a wide range of bacteria.

Furthermore, since the crystal structure has verified that the molecule binds to the ATP binding domain, we may expand the selection of protein targets to include other Mur Ligases such as MurD, MurE and MurF to explore the molecules' multi-targeting capabilities, which will help the molecules evade the development of resistance.

Additional findings elucidated from these studies will provide material evidence that supports their *in vitro* activity against both Gram positives and Gram-negatives.

■ ASSOCIATED CONTENT

The Supporting Information is provided on pages 18-22 of this paper.

SI-1 contains 2D interaction maps from LigPlot+.

■ AUTHOR INFORMATION

Corresponding author

17044263 - Department of Pharmaceutical and Biological Chemistry, UCL School of Pharmacy, 29-39 Brunswick Square, Bloomsbury, London, WC1N 1AX, United Kingdom

Notes

Author declares no competing financial interest.

■ ACKNOWLEDGEMENTS

Special thanks to the OpenSourceAntibiotics team for the helpful discussions and guidance throughout this project.

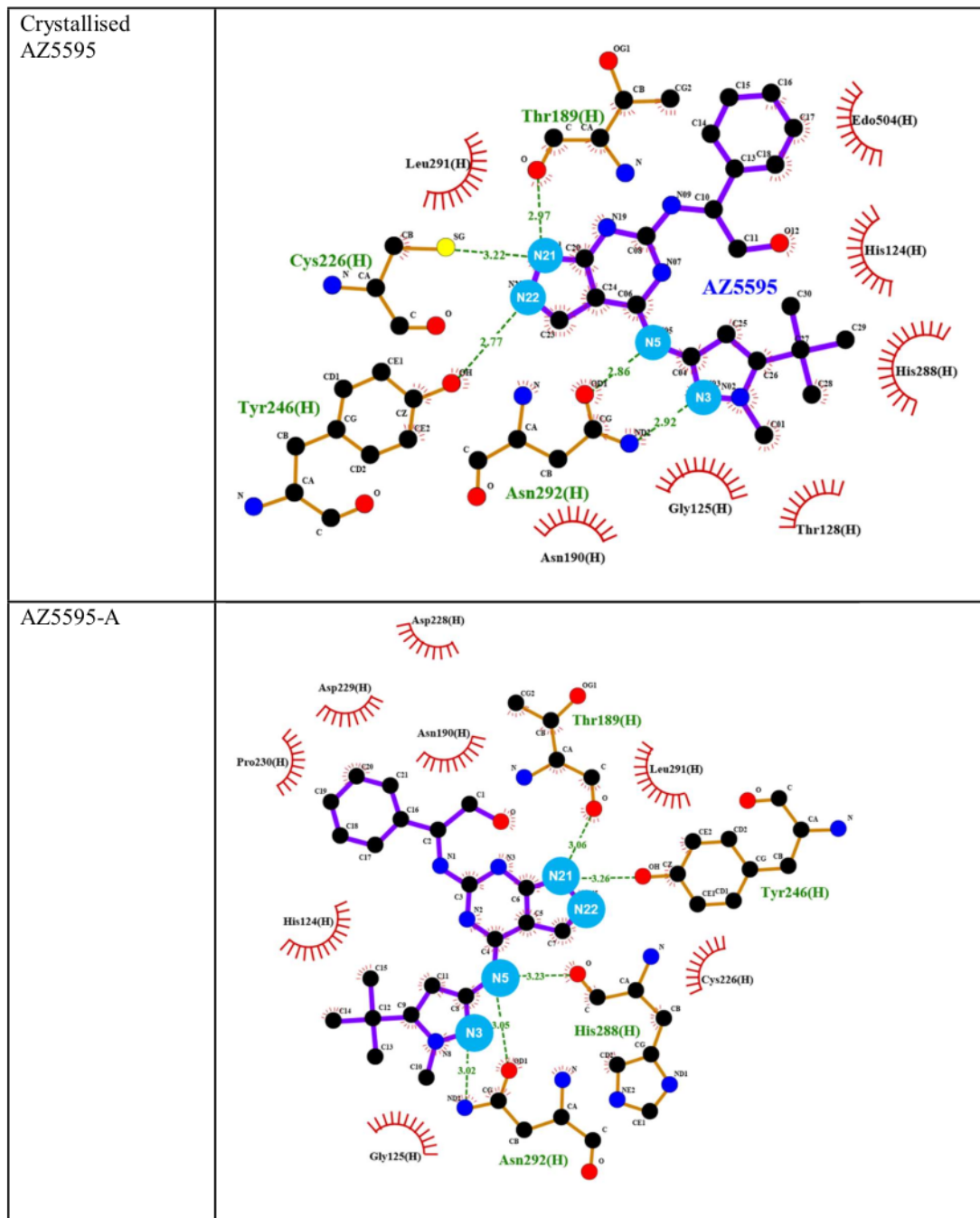
■ REFERENCES

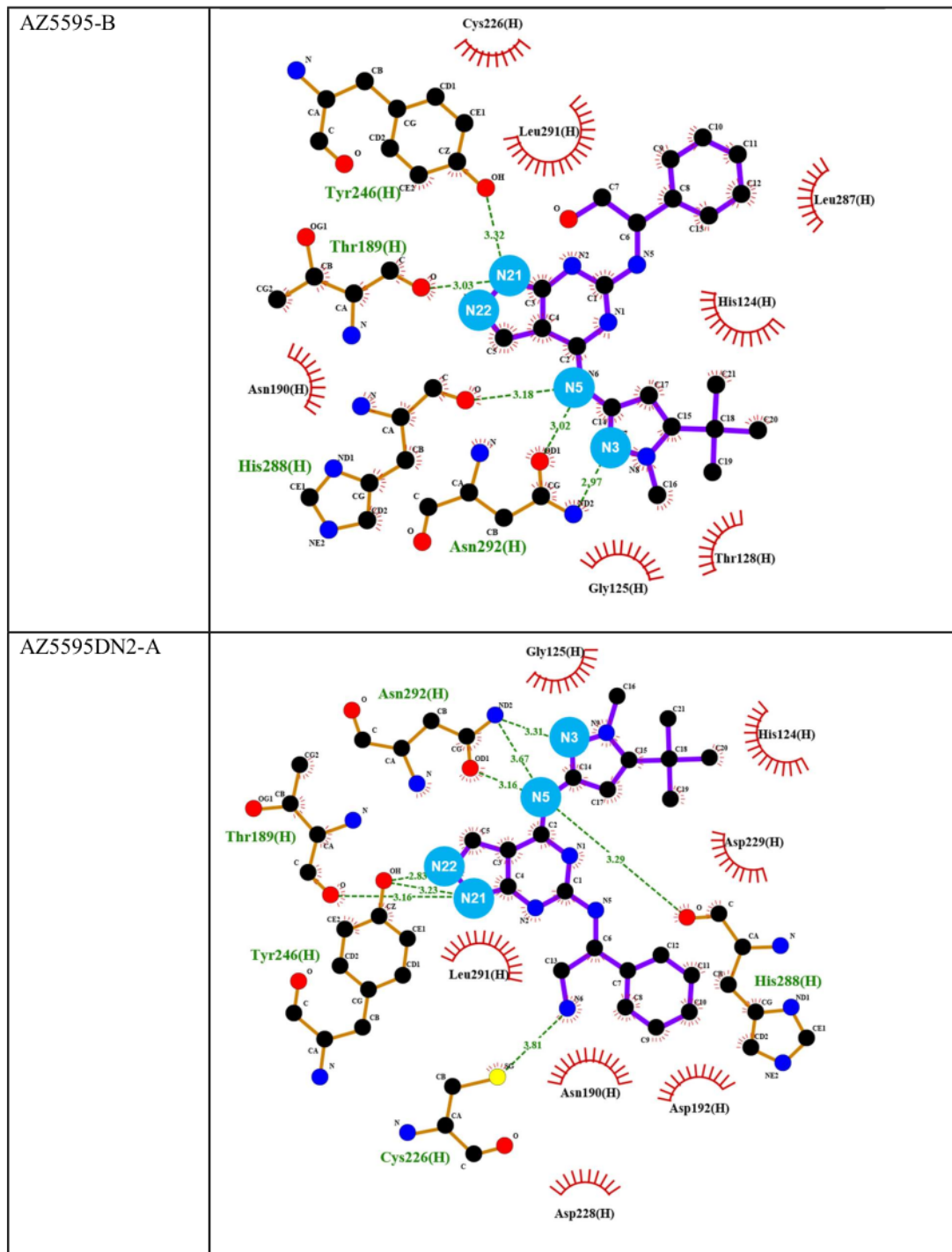
1. NobelPrize.org Sir Alexander Fleming - Nobel Lecture. URL: <https://www.nobelprize.org/prizes/medicine/1945/fleming/lecture/>
2. World Health Organisation, Global Action Plan on Antimicrobial Resistance. **2015**, URL: <https://www.who.int/antimicrobial-resistance/global-action-plan/en/>
3. O'Neill, J., Antimicrobial Resistance: Tackling a crisis for the health and wealth of nations. **2014**, URL: <https://amr-review.org/Publications.html>
4. Silver, L. L., Challenges of antibacterial discovery. *Clin. Microbiol. Rev.* **2011**, 24, 71-109, DOI: <https://doi.org/10.1128/CMR.00030-10>
5. World Health Organisation, Prioritization of pathogens to guide discovery, research and development of new antibiotics for drug resistant bacterial infections, including tuberculosis. **2017**, URL: https://www.who.int/medicines/areas/rational_use/prioritization-of-pathogens/en/
6. Richter, M. F.; Hergenrother, P. J., The challenge of converting Gram-positive-only compounds into broad-spectrum antibiotics. *Ann. N. Y. Acad. Sci.* **2019**, 1435, 18-38, DOI: <https://doi.org/10.1111/nyas.13598>
7. Richter, M. F.; Drown, B. S.; Riley, A. P.; Garcia, A.; Shirai, T.; Svec, R. L.; Hergenrother, P. J., Predictive compound accumulation rules yield a broad-spectrum antibiotic. *Nature* **2017**, 545, 299-304, DOI: <https://doi.org/10.1038/nature22308>
8. Parker, E. N.; Drown, B. S.; Geddes, E. J.; Lee, H. Y.; Ismail, N.; Lau, G. W.; Hergenrother, P. J., Implementation of permeation rules leads to a FabI inhibitor with activity against Gram-negative pathogens. *Nat. Microbiol.* **2020**, 5, 67-75, DOI: <https://doi.org/10.1038/s41564-019-0604-5>
9. Motika, S. E.; Ulrich, R. J.; Geddes, E. J.; Lee, H. Y.; Lau, G. W.; Hergenrother, P. J., Gram-Negative Antibiotic Active Through Inhibition of an Essential Riboswitch. *J. Am. Chem. Soc.* **2020**, 142, 10856-10862, DOI: <https://doi.org/10.1021/jacs.0c04427>
10. Heijenoort, J. v., Recent advances in the formation of the bacterial peptidoglycan monomer unit. *Nat. Prod. Rep.* **2001**, 18, 503-519, DOI: <https://doi.org/10.1039/A804532A>
11. Sangshetti, J. N.; Joshi, S. S.; Patil, R. H.; Moloney, M. G.; Shinde, D. B., Mur Ligase Inhibitors as Anti-bacterials: A Comprehensive Review. *Curr. Pharm. Des.* **2017**, 23, 3164-3196, DOI: <https://doi.org/10.2174/1381612823666170214115048>
12. Smith, C. A., Structure, Function and Dynamics in the mur Family of Bacterial Cell Wall Ligases. *J. Mol. Biol.* **2006**, 362, 640-655, DOI: <https://doi.org/10.1016/j.jmb.2006.07.066>
13. Koudmi, I.; Levesque, R. C.; Paradis-Bleau, C., The biology of Mur ligases as an antibacterial target. *Mol. Microbiol.* **2014**, 94, 242-53, DOI: <https://doi.org/10.1111/mmi.12758>
14. Silver, L. L., Multi-targeting by monotherapeutic antibacterials. *Nat. Rev. Drug Discov.* **2007**, 6, 41-55, DOI: <https://doi.org/10.1038/nrd2202>
15. Tomašić, T.; Šink, R.; Zidar, N.; Fic, A.; Contreras-Martel, C.; Dessen, A.; Patin, D.; Blanot, D.; Müller-Premru, M.; Gobec, S.; Zega, A.; Kikelj, D.; Mašič, L. P., Dual Inhibitor of MurD and MurE Ligases from Escherichia coli and Staphylococcus aureus. *ACS Med. Chem. Lett.* **2012**, 3, 626-630, DOI: <https://doi.org/10.1021/ml300047h>
16. Sova, M.; Kovač, A.; Turk, S.; Hrast, M.; Blanot, D.; Gobec, S., Phosphorylated hydroxyethylamines as novel inhibitors of the bacterial cell wall biosynthesis enzymes MurC to MurF. *Bioorg. Chem.* **2009**, 37, 217-222, DOI: <https://doi.org/10.1016/j.bioorg.2009.09.001>
17. Štrancar, K.; Blanot, D.; Gobec, S., Design, synthesis and structure-activity relationships of new phosphinate inhibitors of MurD. *Bioorg. Med. Chem. Lett.* **2006**, 16, 343-348, DOI: <https://doi.org/10.1016/j.bmcl.2005.09.086>
18. Perdih, A.; Hrast, M.; Barreteau, H.; Gobec, S.; Wolber, G.; Solmajer, T., Benzene-1,3-dicarboxylic acid 2,5-dimethylpyrrole derivatives as multiple inhibitors of bacterial Mur ligases (MurC-MurF). *Bioorg. Med. Chem.* **2014**, 22, 4124-4134, DOI: <https://doi.org/10.1016/j.bmc.2014.05.058>
19. Šink, R.; Kovač, A.; Tomašić, T.; Rupnik, V.; Boniface, A.; Bostock, J.; Chopra, I.; Blanot, D.; Mašič, L. P.; Gobec, S.; Zega, A., Synthesis and

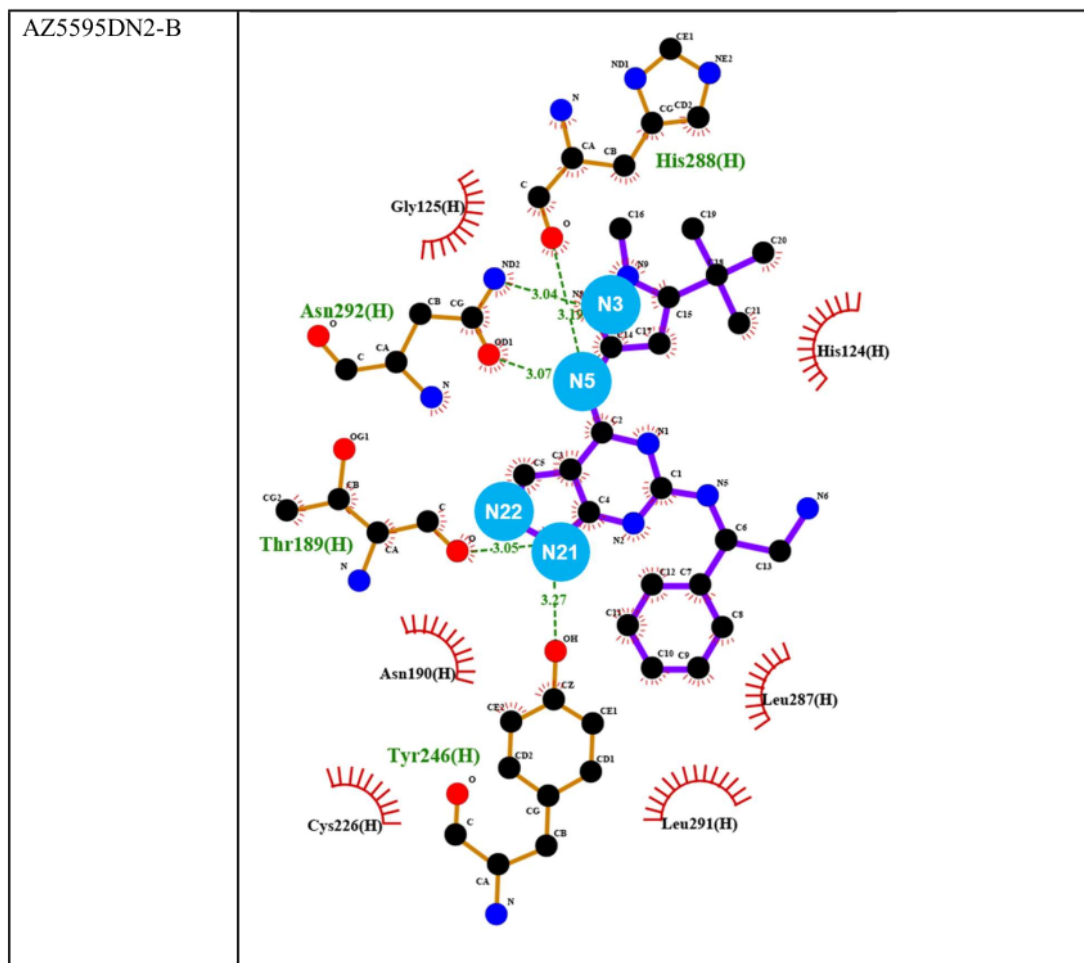
- Biological Evaluation of N-Acylhydrazones as Inhibitors of MurC and MurD Ligases. *ChemMedChem* **2008**, 3, 1362-1370, DOI: <https://doi.org/10.1002/cmde.200800087>
20. Hameed P. S.; Manjrekar, P.; Chinnapattu, M.; Humnabadkar, V.; Shanbhag, G.; Kedari, C.; Mudugal, N. V.; Ambady, A.; de Jonge, B. L. M.; Sadler, C.; Paul, B.; Sriram, S.; Kaur, P.; Gupta, S.; Raichurkar, A.; Fleming, P.; Eyermann, C. J.; McKinney, D. C.; Sambandamurthy, V. K.; Panda, M.; Ravishankar, S., Pyrazolopyrimidines Establish MurC as a Vulnerable Target in *Pseudomonas aeruginosa* and *Escherichia coli*. *ACS Chem. Biol.* **2014**, 9, 2274-2282, DOI: <https://doi.org/10.1021/cb500360c>
21. Meng, X. Y.; Zhang, H. X.; Mezei, M.; Cui, M., Molecular docking: A powerful approach for structure-based drug discovery. *Curr Comput Aided Drug Des* **2011**, 7, 146-157, DOI: 10.2174/157340911795677602
22. Macalino, S. J. Y.; Gosu, V.; Hong, S.; Choi, S., Role of computer-aided drug design in modern drug discovery. *Arch. Pharm. Res.* **2015**, 38, 1686-1701, DOI: <https://doi.org/10.1007/s12272-015-0640-5>
23. Laskowski, R. A.; Swindells, M. B., LigPlot+: Multiple Ligand–Protein Interaction Diagrams for Drug Discovery. *J Chem Inf Model* **2011**, 51, 2778-2786, DOI: <https://doi.org/10.1021/ci200227u>
24. Salentin, S.; Schreiber, S.; Haupt, V. J.; Adasme, M. F.; Schroeder, M., PLIP: fully automated protein–ligand interaction profiler. *Nucleic Acids Res* **2015**, 43, W443-W447, DOI: <https://doi.org/10.1093/nar/gkv315>
25. Schrodinger, LLC, The PyMOL Molecular Graphics System, Version 2.5.0a0. **2015**,
26. Trott, O.; Olson, A. J., AutoDock Vina: improving the speed and accuracy of docking with a new scoring function, efficient optimization, and multithreading. *J. Comput. Chem.* **2010**, 31, 455-461, DOI: <https://doi.org/10.1002/jcc.21334>
27. Morris, G. M.; Huey, R.; Lindstrom, W.; Sanner, M. F.; Belew, R. K.; Goodsell, D. S.; Olson, A. J., AutoDock4 and AutoDockTools4: Automated docking with selective receptor flexibility. *J. Comput. Chem.* **2009**, 30, 2785-2791, DOI: <https://doi.org/10.1002/jcc.21256>
28. Wang, Z.; Sun, H.; Yao, X.; Li, D.; Xu, L.; Li, Y.; Tian, S.; Hou, T., Comprehensive evaluation of ten docking programs on a diverse set of protein–ligand complexes: the prediction accuracy of sampling power and scoring power. *Phys. Chem. Chem. Phys.* **2016**, 18, 12964-12975, DOI: <https://doi.org/10.1039/C6CP01555G>
29. Trott, O. Vina Video Tutorial. URL: <http://vina.scripps.edu/tutorial.html>
30. RCSB PDB Small Molecule Ligands. <http://pdb101.rcsb.org/learn/guide-to-understanding-pdb-data/small-molecule-ligands>
31. Chen, Y.-C., Beware of docking! *Trends Pharmacol. Sci.* **2015**, 36, 78-95, DOI: <https://doi.org/10.1016/j.tips.2014.12.001>
32. Pantsar, T.; Poso, A., Binding Affinity via Docking: Fact and Fiction. *Molecules* **2018**, 23, 1899, DOI: <https://doi.org/10.3390/molecules23081899>
33. Trott, O.; Olson, A. J. AutoDock Vina Manual. URL: <http://vina.scripps.edu/manual.html>
34. Boström, J.; Norrby, P.-O.; Liljefors, T., Conformational energy penalties of protein-bound ligands. *J. Comput. Aided Mol. Des.* **1998**, 12, 383-383, DOI: <https://doi.org/10.1023/A:1008007507641>
35. Vieth, M.; Hirsh, J. D.; Brooks, C. L., Do active site conformations of small ligands correspond to low free-energy solution structures? *J. Comput. Aided Mol. Des.* **1998**, 12, 563-572, DOI: <https://doi.org/10.1023/A:1008055202136>
36. Wang, Q.; Pang, Y.-P., Preference of Small Molecules for Local Minimum Conformations when Binding to Proteins. *PLOS ONE* **2007**, 2, e820, DOI: <https://doi.org/10.1371/journal.pone.0000820>

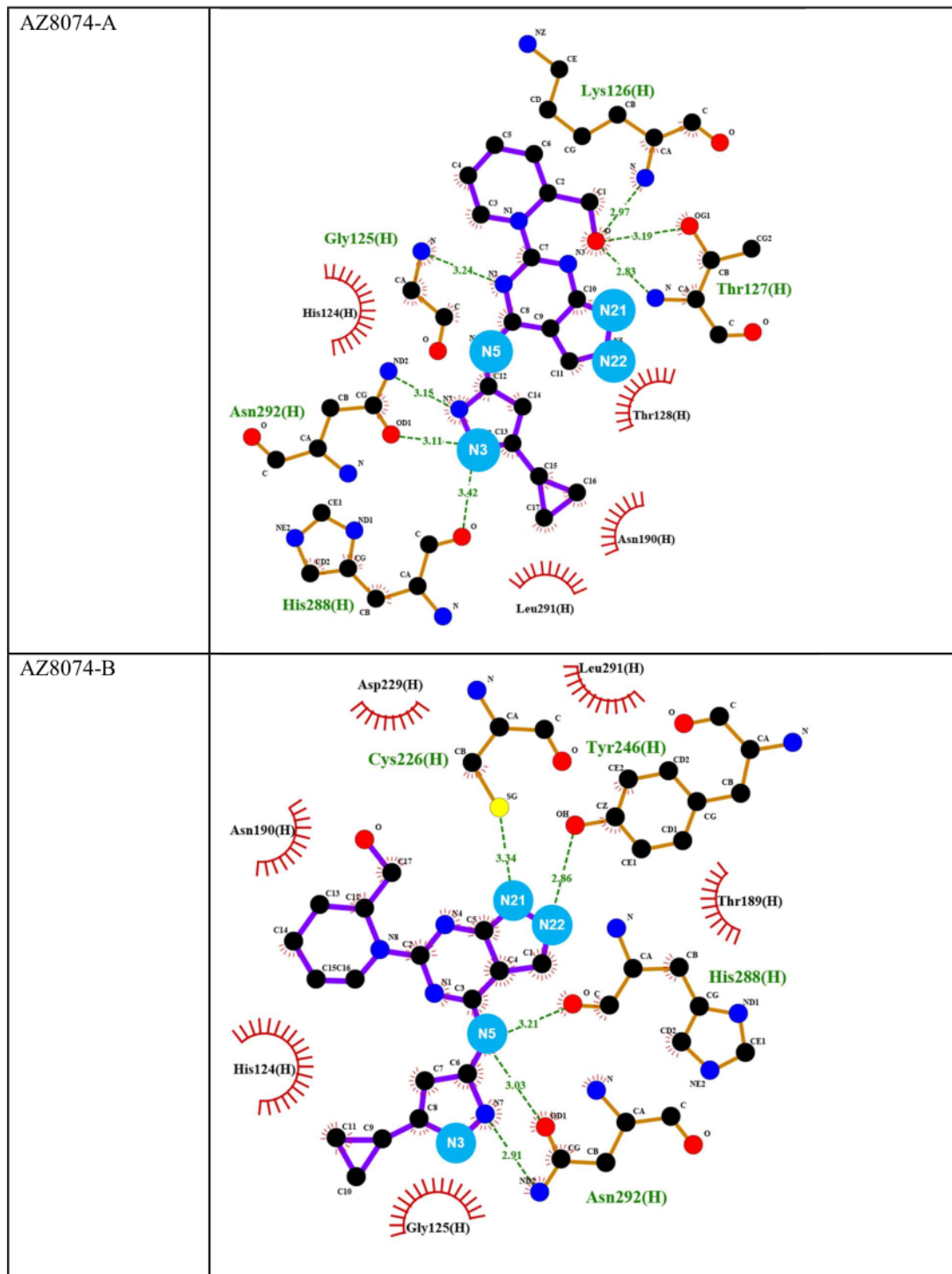
■ Supporting Information

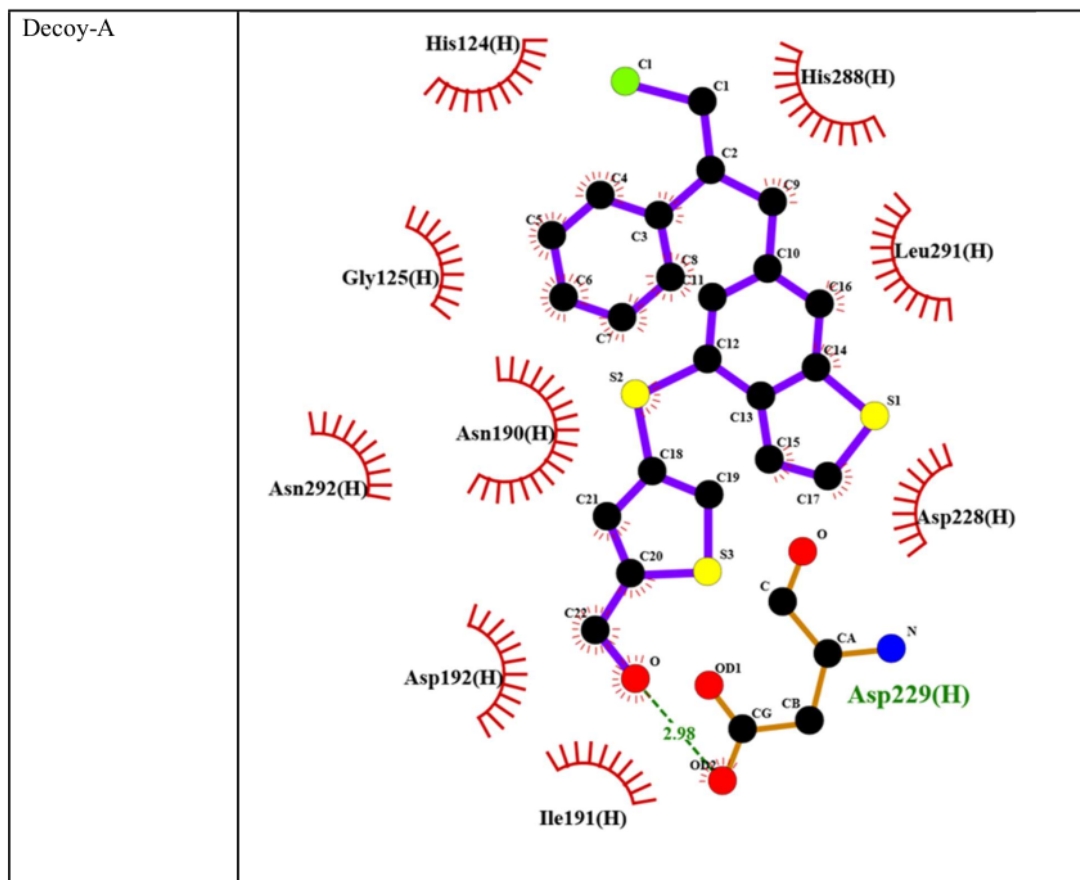
SI-1 This section includes 2D images of the interaction maps from LigPlot+ used to analyse the binding interactions and distances in **Binding Interactions and Distances Profile**.











17044263_ResearchPaper

GRADEMARK REPORT

FINAL GRADE

/100

GENERAL COMMENTS

Instructor

PAGE 1

PAGE 2

PAGE 3

PAGE 4

PAGE 5

PAGE 6

PAGE 7

PAGE 8

PAGE 9

PAGE 10

PAGE 11

PAGE 12

PAGE 13

PAGE 14

PAGE 15

PAGE 16

PAGE 17

PAGE 18

PAGE 19

PAGE 20

PAGE 21

PAGE 22
